Supplementary Information

Structural recognition and stabilization of tyrosine hydroxylase by the J-domain protein DNAJC12

Mary Dayne S. Tai[1,2], Lissette Ochoa[3], Marte I. Flydal[1,4], Lorea Velasco[5], Jimena Muntaner[3], César Santiago[3], Kunwar Jung-KC[1,2,6], Fernando Moro[5], Juha P. Kallio[1], Arturo Muga[5], José María Valpuesta[3,7,*], Jorge Cuéllar[3,*], Aurora Martinez[1,2,6,*]

[1]Department of Biomedicine, University of Bergen, Bergen, Norway.
[2]Neuro-SysMed Center, Department of Neurology, Haukeland University Hospital, Bergen, Norway.
[3]Centro Nacional de Biotecnología (CNB-CSIC), Madrid, Spain.
[4]Department of Medical Genetics, Haukeland University Hospital, 5021, Bergen, Norway.
[5]Instituto Biofisika (UPV/EHU, CSIC), Universidad del País Vasco, (UPV/EHU), and Departamento de Bioquímica y Biología Molecular, Facultad de Ciencia y Tecnología, Universidad del País Vasco, (UPV/EHU), Barrio Sarriena, 48940 Leioa, Spain.
[6]K.G Jebsen Center for Translational Research in Parkinson's Disease, University of Bergen, Bergen, Norway.
[7]Unidad de Nanobiotecnología, CNB-CSIC-IMDEA Nanociencia Associated Unit, 28049 Madrid, Spain

*Co-corresponding authors: José María Valpuesta, jmv@cnb.csic.es; Jorge Cuéllar, jcuellar@cnb.csic.es; Aurora Martinez, aurora.martinez@uib.no.

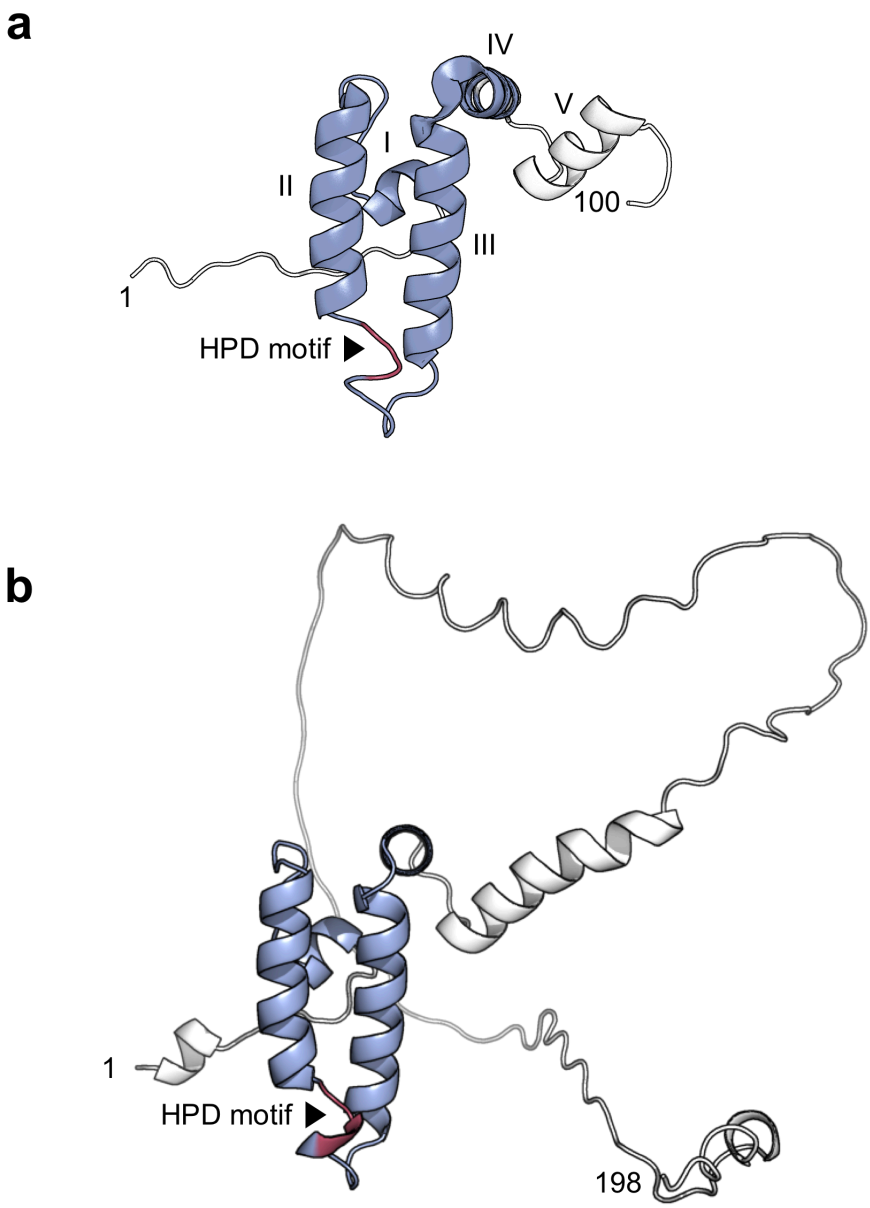

Supplementary Figure 1. Partial NMR (PDB 2CTQ) and full-length AlphaFold predicted structures of human DNAJC12.

a, The NMR-solved structure of the first 100 resides of DNAJC12 shows an unstructured 13-residue N-terminal tail, the characteristic tetra-helical structure (labelled as helices I-IV) of the J-domain (JD) and an additional fifth helix (labelled as helix V). **b**, AlphaFold (Jumper et al. Nature **596**, 583-589 (2021)) predicts the extended conformation of DNAJC12. In both figures the JD is shown in blue, with the His-Pro-Asp (HPD) motif in red.

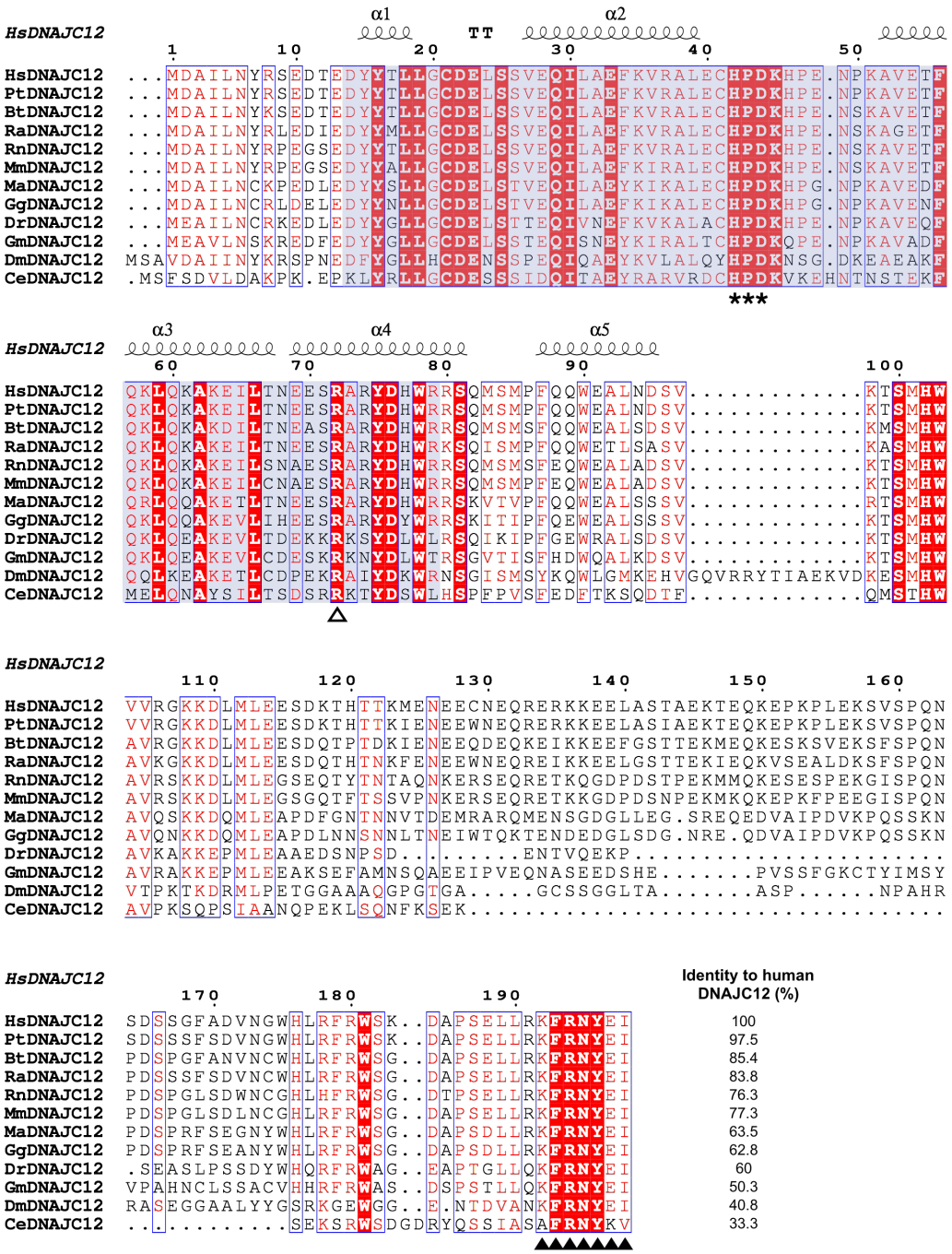

Supplementary Figure 2. Sequence alignment of DNAJC12 from different species.

Sequence alignment performed with Clustal Omega (McWilliam et al. Nucleic Acids Res **41**, W597-600 (2013)) and visualized with ESPript (Robert and Gouet. Nucleic Acids Res. **42**, W320-4 (2014)). Residues strictly conserved across all sequences are marked with red background, and residues in red letters are above the Similarity Global Score of 0.7. The aligned sequences are from *Homo sapiens* (Hs; NP_068572.1), *Pan troglodytes* (Pt; XP_521687.2), Bos taurus (Bt; NP_776521.1), Rousettus aegyptiacus (Ra; XP_015985286.2), *Rattus norvegicus* (Rn; NP_001029204.1), *Mus musculus* (Mm; NM_013888.3), *Motacilla alba* (Ma; XP_037996268.1), *Gallus gallus* (Gg; NP_001186459.1), Danio rerio (Dr; NP_001314717.1), Gadus morhua (Gm; XP_030235349.1), *Drosophila melanogaster* (Dm; NP_651807.1), *Caenorhabditis elegans* (Ce; NP_001023271.1). The C-terminal heptapeptide sequence KFRNYEI is conserved beyond vertebrates (black triangles), while FRNY is already present in *Caenorhabditis elegans*. The J-domain is highlighted in gray, while the HPD motif is marked with asterisks. Arg72, which is mutated in some patients with DNAJC12 deficiency, is conserved in all DNAJC12 homologues and is marked with a white triangle.

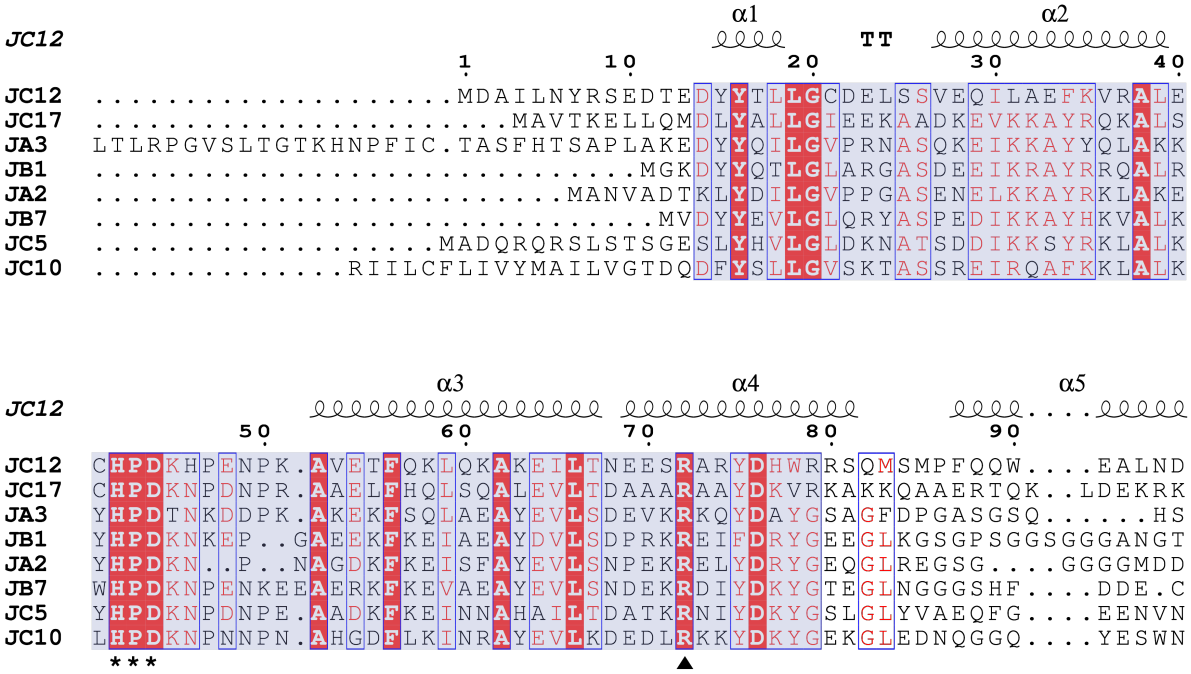

Supplementary Figure 3. Sequence alignment of the J-domain from different human JDPs.

Sequence alignment performed with Clustal Omega (McWilliam et al. Nucleic Acids Res **41**, W597-600 (2013)) and visualized with ESPript (Robert & Gouet. Nucleic Acids Res **42**, W320-4 (2014)). Residues strictly conserved across all sequences are marked with red background and red letters are above the Similarity Global Score of 0.7. The JD is highlighted in gray, while the HPD motif is marked with asterisks. Arg72 is also conserved in the selected human JDPs and is marked with a triangle. The aligned sequences are DNAJC12 (NP_068572.1), DNAJC17 (NP_060633.1), DNAJA3 (NP_001128582.1), DNAJB1 (NP_001287843.1), DNAJA2 (NP_005871.1), DNAJB7 (NP_660157.1), DNAJC5 (NP_079495.1), DNAJC10 (NP_001258510.1).

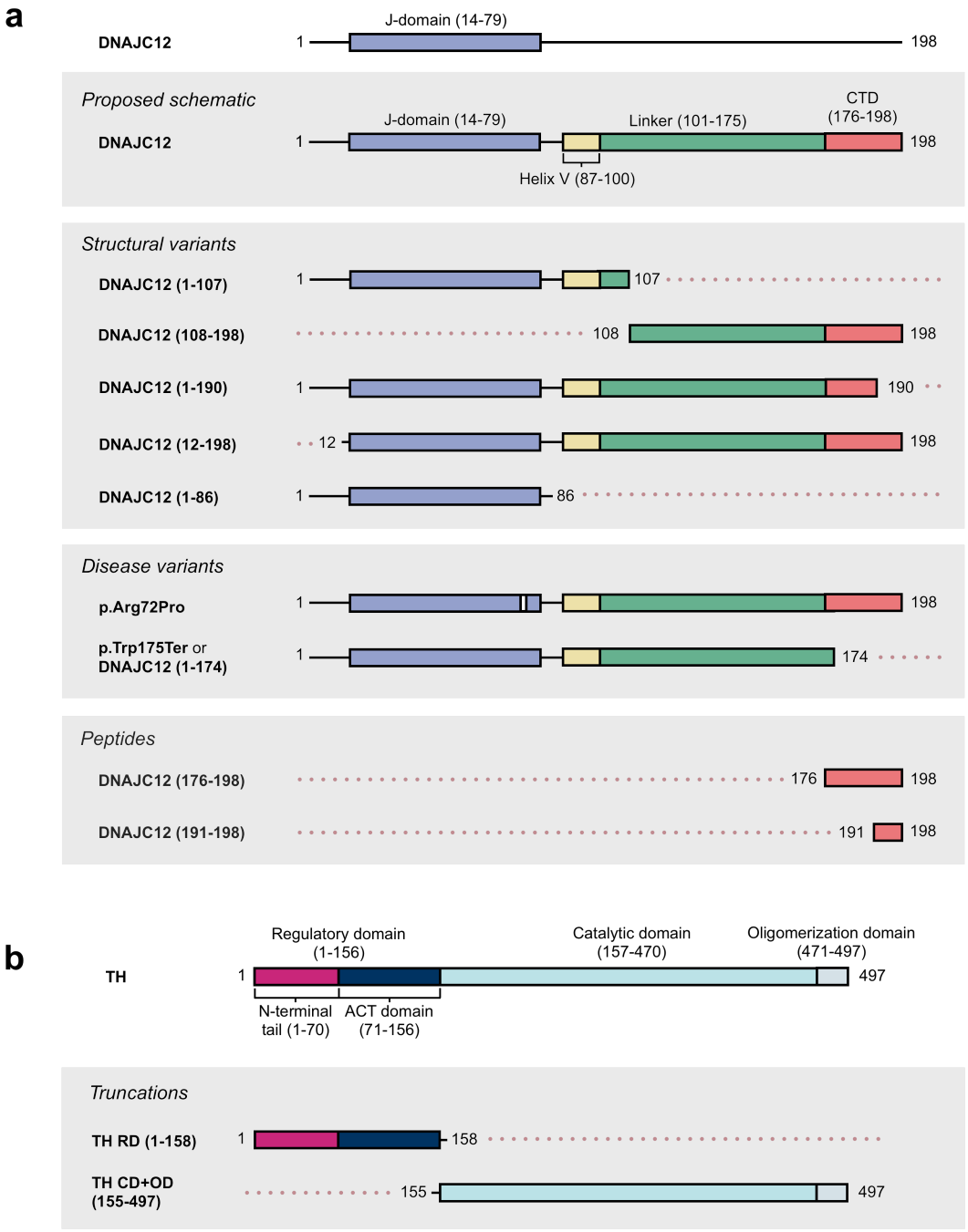

Supplementary Figure 4. Schematic representation of all DNAJC12 and TH variants and peptides used in this study.

a, Schematic representation of DNAJC12 isoform a and variants prepared. The proposed additional functional regions in the full-length DNAJC12 sequence in addition to the J-domain (blue), i.e., the linker (including helix V (yellow), defined using the DNAJC12 model by AlphaFold; green) and the client-binding C-terminal domain (CTD; red), are also annotated in the schematic representation. **b,** Schematic representation of full-length TH and truncated variants used in this study**.** TH is composed of the regulatory domain that contains the N-terminal tail (magenta) and an ACT domain (dark blue), followed by the catalytic (light blue) and oligomerization domains (light gray).

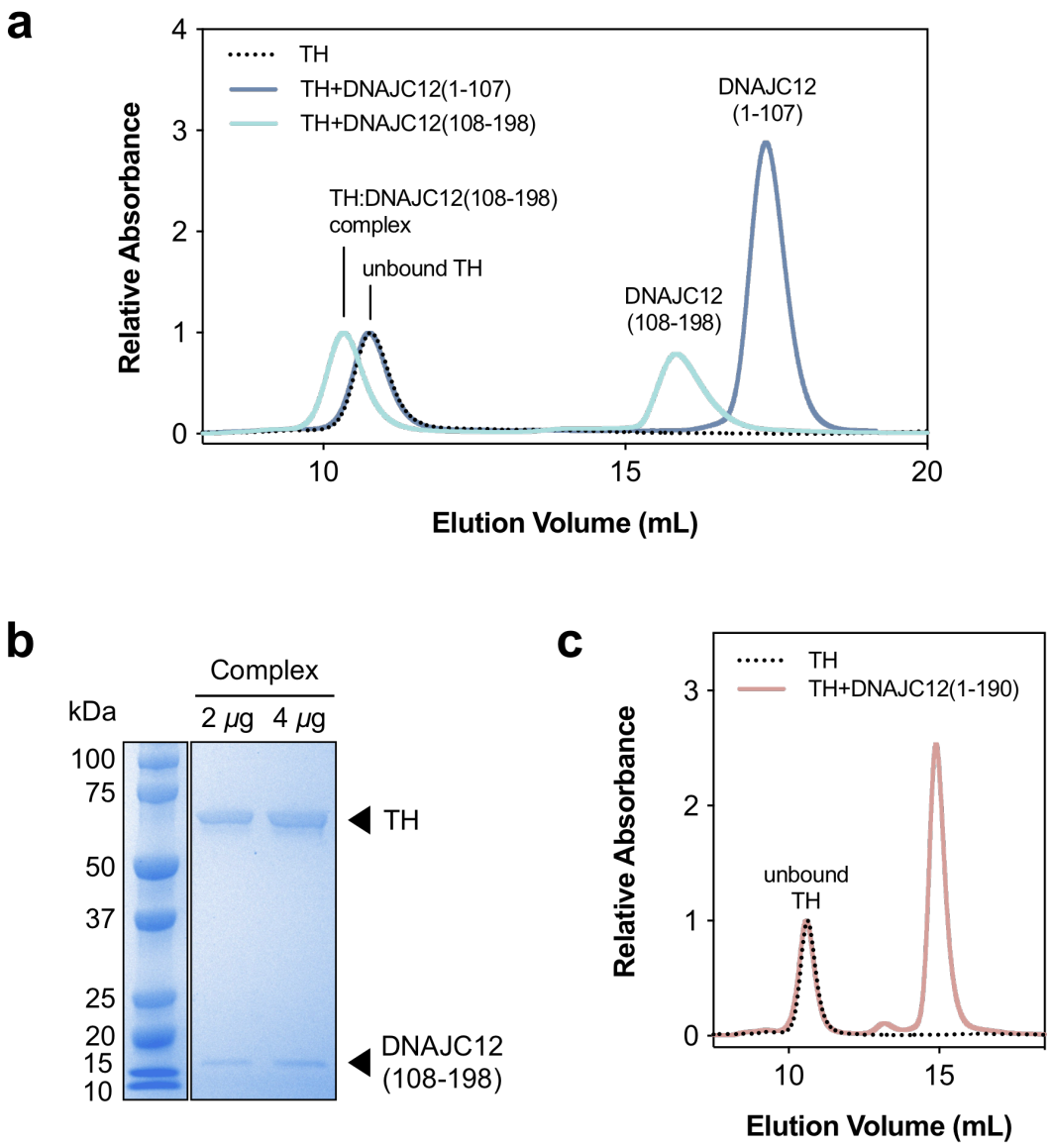

Supplementary Figure 5. Interaction analyses of truncated variants of DNAJC12 to TH.

a, SEC analyses of samples containing a 1:16 TH tetramer:DNAJC12 monomer ratio of TH:DNAJC12(1-107) or TH:DNAJC12(108-198), compared with a sample containing TH only on a Superdex™ 200 Increase 10/300 GL column. The addition of the DNAJC12(108-198) (light blue), but not DNAJC12(1-107) (dark blue), shifts the elution of TH (stippled line) to an earlier volume, indicating the binding of the C-terminal section to TH. **b,** SDS-PAGE of the collected protein samples eluting in the putative complex peak (in **a**), showing the co-elution of TH and DNAJC12(108-198) (~10.5 kDa) in this peak. **c**, SEC analyses of TH alone (stippled line) and with DNAJC12(1-190) (red) at a 1:16 TH tetramer:DNAJC12 monomer ratio on a Superdex™ 200 Increase 10/300 GL column, showing that the removal of the evolutionarily conserved C-terminal region in DNAJC12 abolishes its ability to bind to TH.

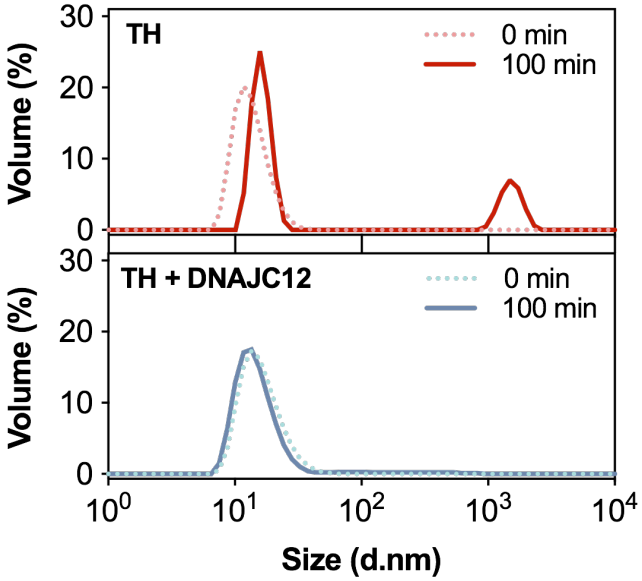

Supplementary Figure 6. Particle size distribution (by % volume) measured by dynamic light scattering (DLS).

Size distribution (diameter; d.nm) for TH alone (red) and in the presence of DNAJC12 (blue) at 0 min (stippled lines) and after 100 min incubation (solid lines) at 37 ºC.

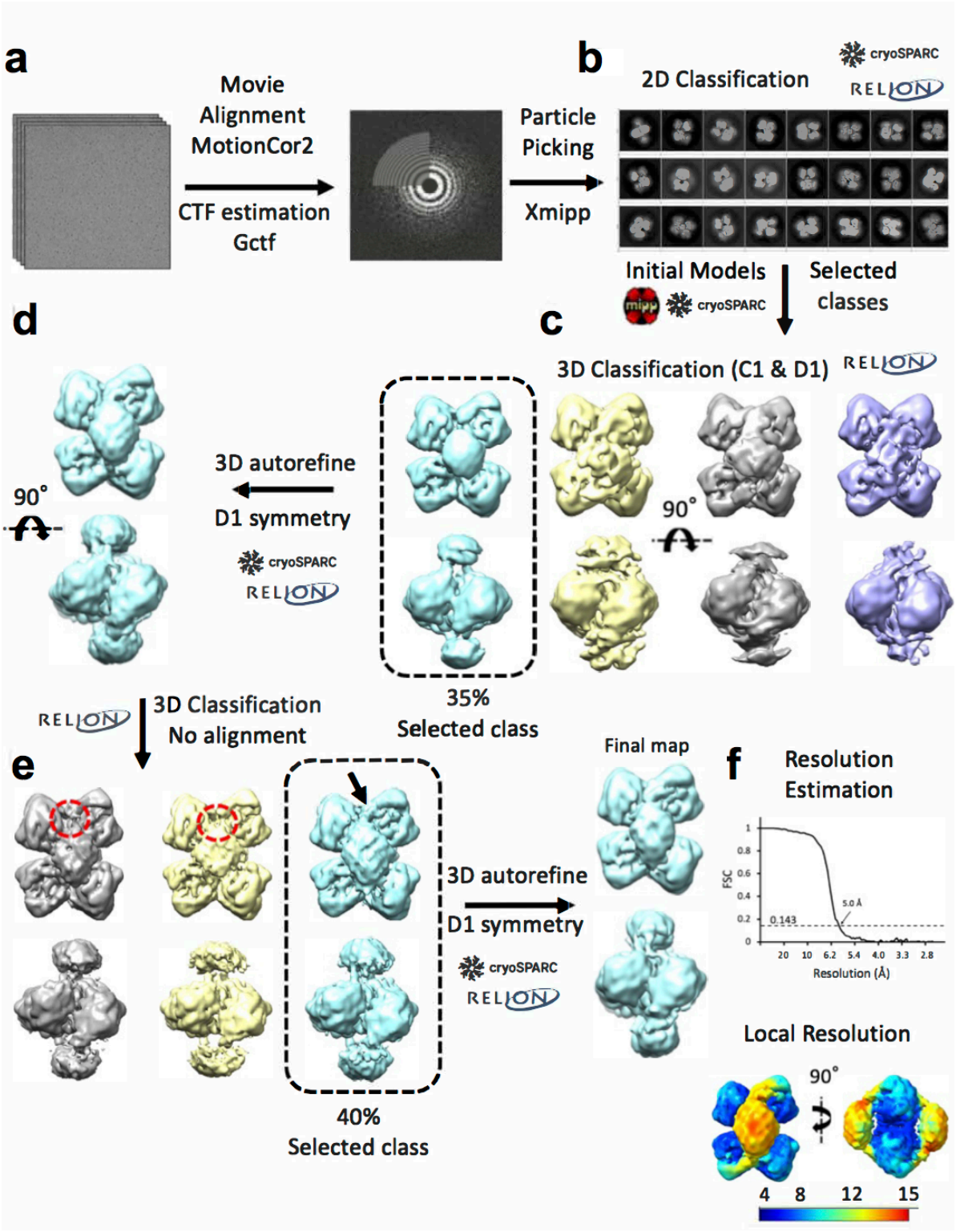

Supplementary Figure 7. Workflow of the 3D reconstruction procedure.

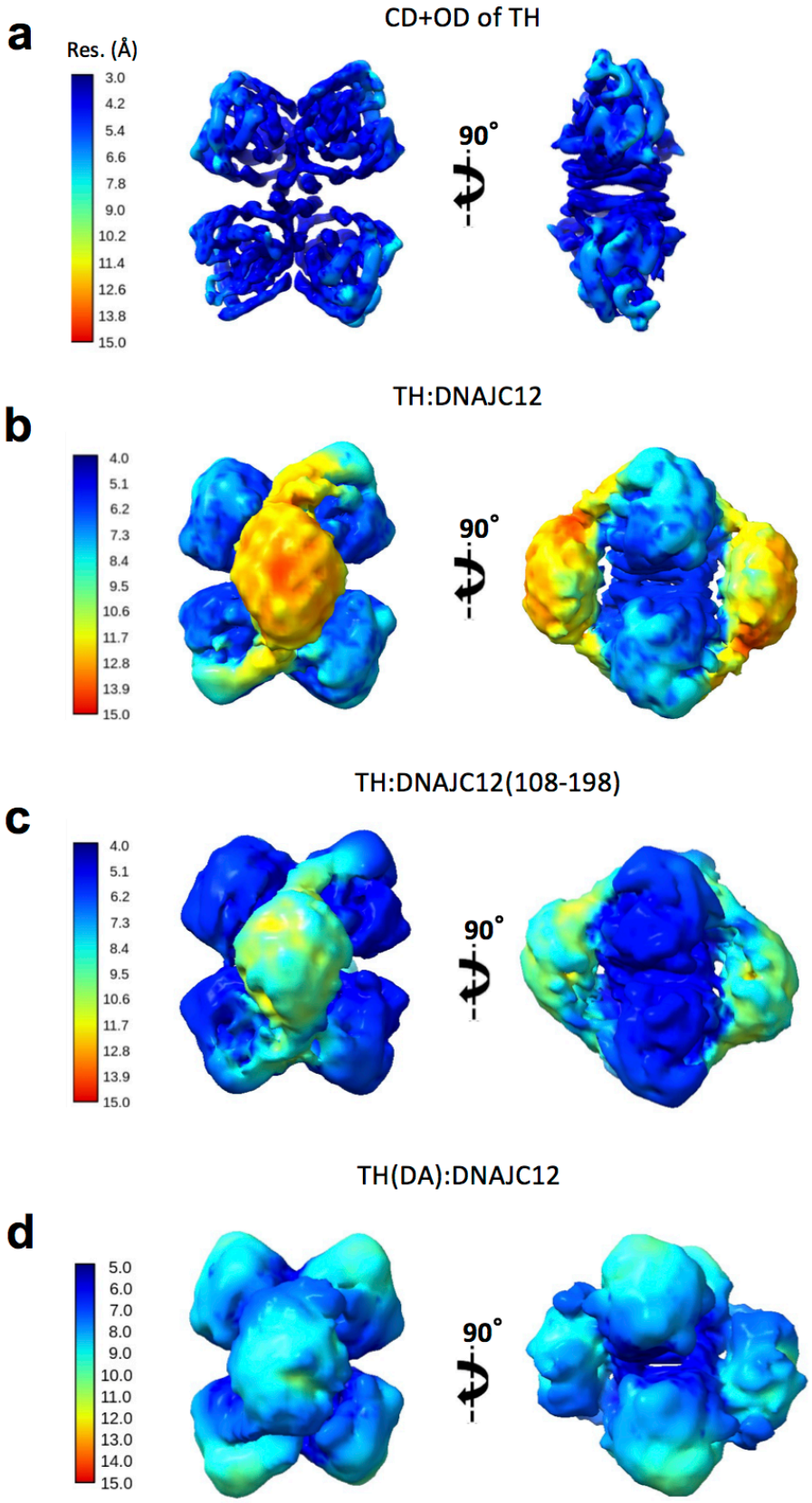

Supplementary Figure 8. Anisotropy in the resolution of the three 3D reconstructions.

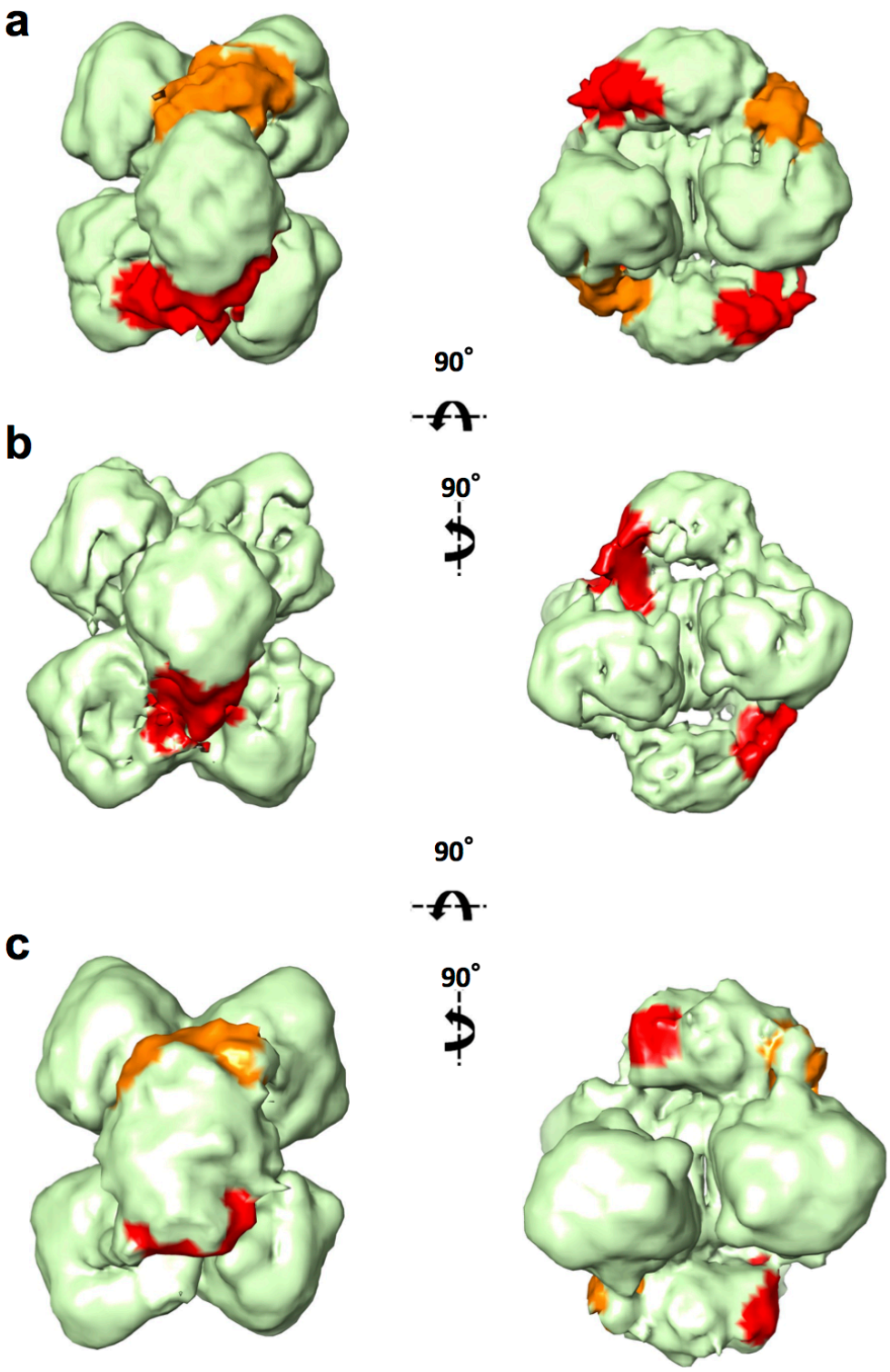

Supplementary Figure 9. Two different views of the three 3D reconstructions obtained in this work, the TH:DNAJC12 (a), TH:DNAJC12(108-198) (b) and TH(DA):DNAJC12 (c) complexes.

The yellow and red colored masses correspond to the volumes assigned to the J-domain and C-terminal domain, respectively (see images in Fig. 4b, d and f).

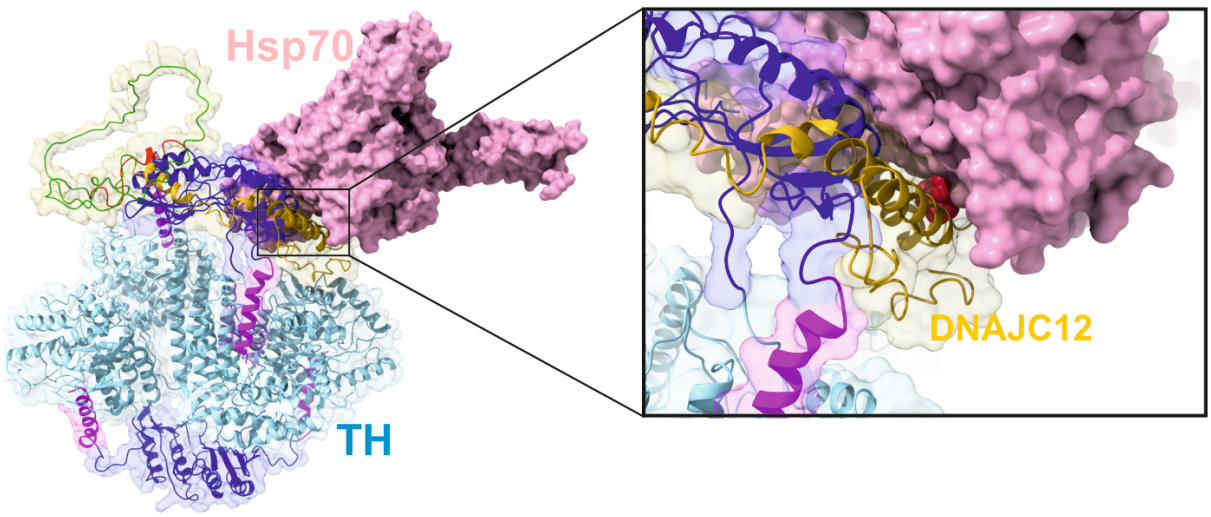

Supplementary Figure 10. Model of the interaction of the TH:DNAJC12 complex with Hsp70, through the DNAJC12 HPD motif.

A combined ribbon and surface model of the TH:DNAJC12 complex is superimposed on the experimental model of Hsp70 of *Escherichia coli* (DnaK) with bound J-domain (JD; PDB 5NRO), shown in surface representation. JDs from both models have been aligned using ChimeraX software. For clarity, the JD from *E. coli* has been excluded from PDB 5NRO after structural alignment. The catalytic domain (CD) and regulatory domain (RD) of TH are shown in cyan and blue, respectively. Additionally, the inset highlights DNAJC12 JD (colored in gold) bound to Hsp70, emphasizing the HPD binding motif shown as red spheres.

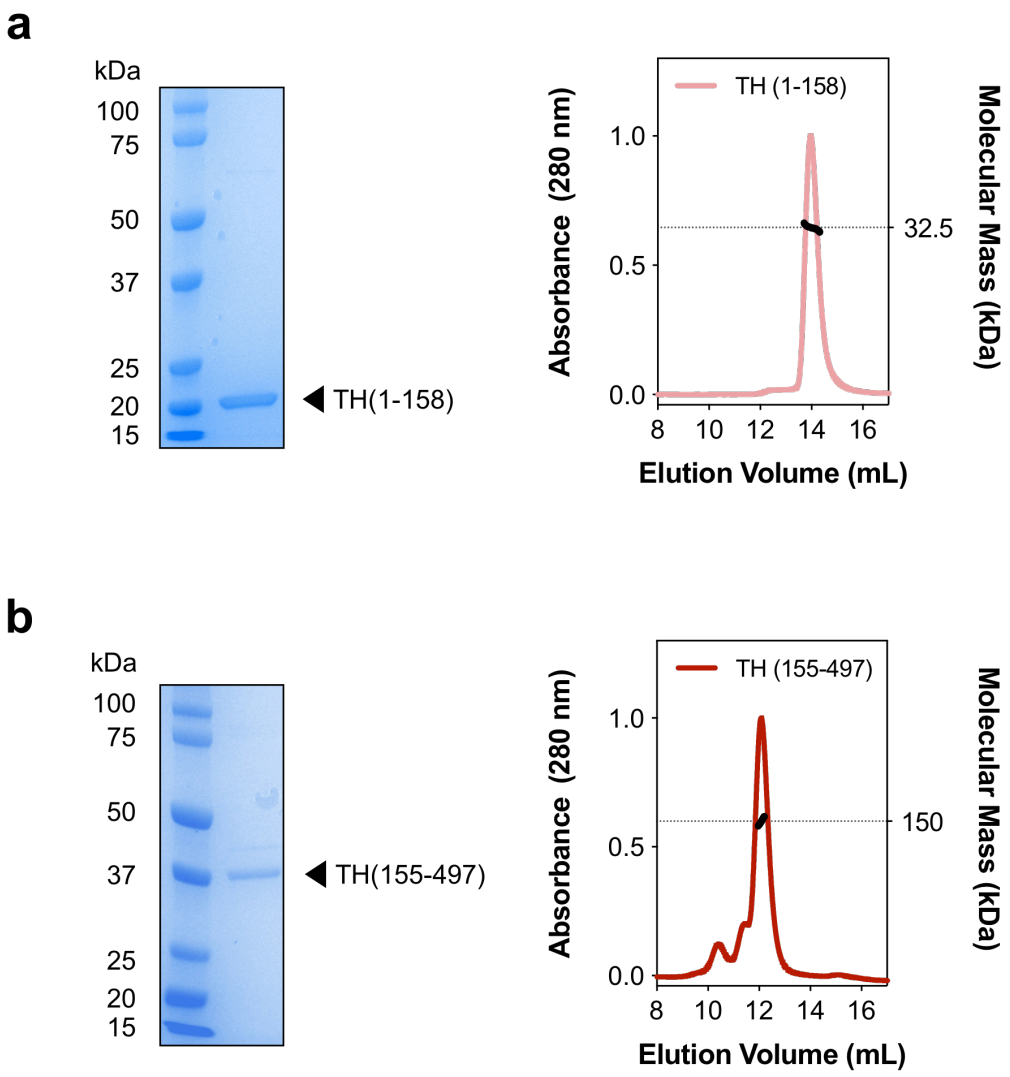

Supplementary Figure 11. Characterization of the oligomeric distribution of isolated TH domains.

a, SDS-PAGE (left) of the purified regulatory domain (RD; residues 1-158), showing the correct theoretical monomeric size of the RD (~17 kDa). Analysis by SEC-MALS (right) confirmed that the RD was dimeric (32.5 ± 0.17 kDa). **b,** SDS-PAGE analysis (left) of the purified catalytic and oligomerization domains (CD+OD; residues 155-497) also showing the correct monomeric size of the CD+OD (~38 kDa). Subsequent SEC-MALS analysis determined that the CD+OD was tetrameric (150 ± 0.099 kDa).

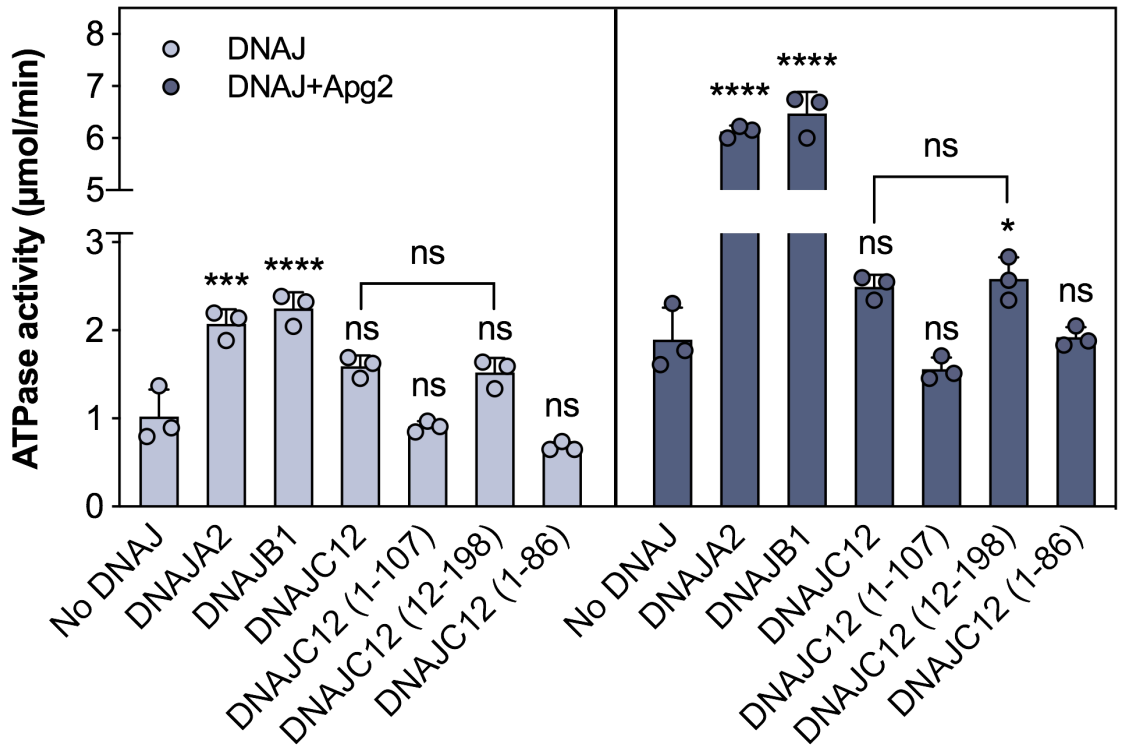

Supplementary Figure 12. Comparison of Hsc70 stimulation by truncated DNAJC12 variants with and without Apg2.

The ability of truncated DNAJC12 variants to stimulate Hsc70 ATPase activity was compared to that of DNAJA2 and DNAJB1. The data represent the mean ± SD for n=3 independent experiments. The ATPase activity of Hsc70 recorded with the different JDPs was compared to their respective controls (either with (dark blue) or without Apg2 (light purple)), that only have Hsc70 and do not contain any JDP, by one-way ANOVA and Tukey's post-hoc test (*p=0.0245; ***p=0.0001; ****p<0.0001). A small statistically-significant increase in Hsc70 ATPase activity was recorded in the presence of the DNAJC12 variant lacking the N-terminal tail, DNAJC12(12-198). However, using the same multiple comparison analysis, there was no significant difference found in the Hsc70 ATPase activities recorded in the presence of full-length DNAJC12 or DNAJC12(12-198).

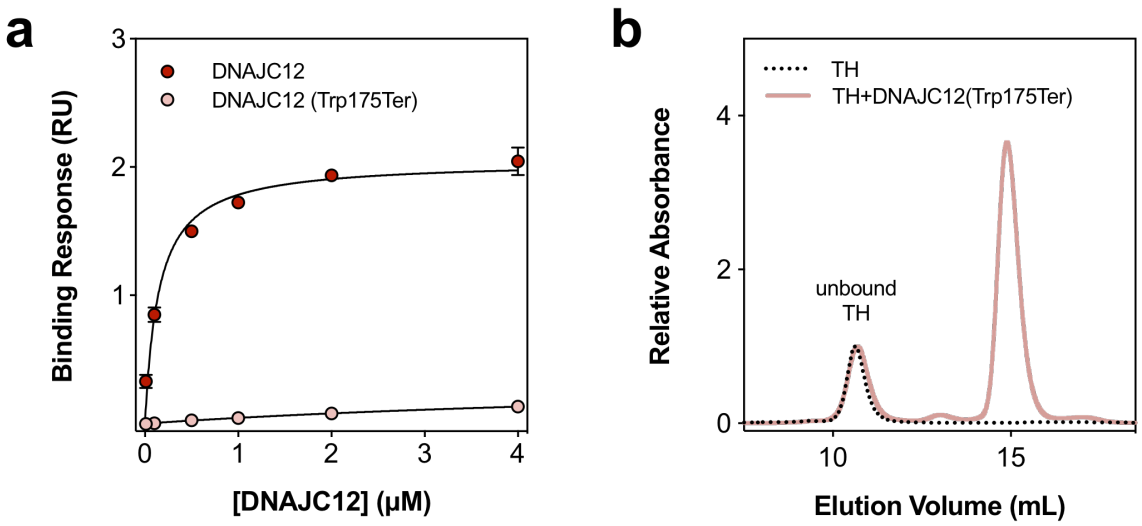

Supplementary Figure 13. Interaction analyses of the disease-associated variant DNAJC12(Trp175Ter) to TH.

a, Binding analyses of DNAJC12(Trp175Ter) to TH by BLI. Binding responses to immobilized TH were recorded at 0, 0.1, 0.5, 1, 2 and 4 µM DNAJC12, full-length (red) or DNAJC12(Trp175Ter) (pink). Unlike the control samples with TH and full-length DNAJC12, no binding response was measured for the disease variant. The binding responses are presented as mean ± 95% CI for 3 independent samples, and the fitting to a non-linear regression curve provided K_D values of 153 ± 44 nM for full-length DNAJC12. **b**, SEC analyses of samples containing a 1:16 molar ratio of TH tetramer:DNAJC12(Trp175Ter) monomer compared with a sample containing TH alone**.** The addition of the DNAJC12(Trp175Ter) (pink line), does not shift the elution of TH (black stippled line) to an earlier volume, indicating that the two proteins do not form a complex.

Supplementary Table 1. Summary of K_D values derived by BLI.

The effect of truncations and dopamine (DA) treatment on the binding affinity of the TH:DNAJC12 interaction was studied by bio-layer interferometry (BLI). Values represent the mean ± SD of K_D calculated from the non-linear fitting of binding responses recorded from n=3 independent experiments. The K_D values derived using truncated DNAJC12 or TH variants, or DA treatment, were compared to the calculated K_D of the wild-type TH:DNAJC12 interaction. Significant differences between samples were determined by one-way ANOVA and Tukey's post-hoc HSD test.

TH	DNAJC12	K_D (mean ± SD)	Adjusted p-value	Significance
wild-type	wild-type	148.07 ± 13.01 µM	-	-
wild-type	(108-198)	43.27 ± 10.75 µM	0.0003	***
wild-type	(176-198)	152.53 ± 13.75 µM	0.9979	ns
wild-type + DA	wild-type	131.50 ± 17.50 µM	0.7938	ns
RD (1-158)	(176-198)	158.57 ± 29.41 µM	0.9497	ns

Supplementary Table 2. Parameters for cryoEM data collection.

Data collection	TH:DNAJC12 EMD-18047	TH:DNAJC12(108-198) EMD-18058	TH(DA):DNAJC12 EMD-18289
Microscope	FEI Titan Krios	FEI Titan Krios	FEI Titan Krios
Voltage (keV)	300	300	300
Detector	Gatan K3	Gatan K3	Gatan K3
Nominal magnification	105,000x	105,000x	105,000x
Pixel size (Å)	0.85	0.85	0.85
Defocus range (μm)	-1.0 to -2.6	-1.0 to -2.6	-1.0 to -2.6
Exposure time (s)	1	1	1
Electron dose ($e^-/Å^2$)	40-42	40-42	40-42
Frames	40	40	40
Dose/frame ($e^-/Å^2$)	1	1	1
Movies (no.)	12,996	18,329	12,826
Initial particles (no.)	2,602,997	1,283,996	2,474,620
Final particles (no.)	74,638	128,537	46,555
Final resolution (Å)	D1	D1	D1
	5.7	5	5.7

Supplementary Table 3. Crosslinking-MS analysis of TH:DNAJC12, TH:DNAJC12(108-198), TH:DNAJC12(176-198), TH(DA):DNAJC12 and TH RD:DNAJC12 complexes.

Peptides identified by XL-MS containing sequences from both TH and DNAJC12 are listed below, with the first peptide from DNAJC12 and the second from TH. The peptide sequence and the positions of the first and last residues of each peptide are indicated, while the crosslinking sites are highlighted in bold letters. The peptide pairs are organized by their location within DNAJC12 (either the J-domain (JD), linker or the C-terminal domain (CTD)) and whether they were found in the full-length TH samples with and without dopamine (DA) or in the truncated TH form containing only the regulatory domain (RD).

		TH	TH (DA)	RDs (TH)
DNAJC12	JD	^{62}A**K**EILTNEESR^{72}–^{17}AVSELDA**K**QAEAIMSPR^{33}	^{62}A**K**EILTNEESR^{72}–^{17}AVSELDA**K**QAEAIMSPR^{33}	^{62}A**K**EILTNEESR^{72}–^{99}AV**K**VFETFEAK^{109}
		^{62}A**K**EILTNEESR^{72}–^{90}AT**K**PSALSR^{98}	^{62}A**K**EILTNEESR^{72}–^{90}AT**K**PSALSR^{98}	^{62}A**K**EILTNEESR^{72}–^{90}AT**K**PSALSR^{98}
			^{62}A**K**EILTNEESR^{72}–^{99}AV**K**VFETFEAK^{109}	
			^{62}A**K**EILTNEESR^{72}–^{204}**K**LIAEIAFQYR^{214}	
			^{81}SQMSMPFQQWEALNDSV**K**TSMHWVVR^{106}–^{157}SPAGP**K**VPWFPR^{168}	
	Linker	^{134}ER**K**^{136}–^{90}AT**K**PSALSR^{98}	^{136}K**K**EELASTAEK^{146}–^{90}AT**K**PSALSR^{98}	^{137}**K**EELASTAEK^{146}–^{99}AV**K**VFETFEAK^{109}
		^{134}ER**K**^{136}–^{17}AVSELDA**K**QAEAIMSPR^{33}	^{109}**K**DLMLEESDK^{118}–^{157}SPAGP**K**VPWFPR^{168}	
		^{134}ER**K**^{136}–^{204}**K**LIAEIAFQYR^{214}	^{119}THTT**K**MENEEBNEQR^{133}–^{90}AT**K**PSALSR^{98}	
		^{147}TEQ**K**^{150}–^{234}EVYTTL**K**^{240}		
	CTD	^{181}WS**K**DAPSELLR^{191}–^{47}**K**ER^{49}	^{181}WS**K**DAPSELLR^{191}–^{77}EG**K**AMLNLLFSPR^{89}	^{181}WS**K**DAPSELLR^{191}–^{77}EG**K**AMLNLLFSPR^{89}
		^{181}WS**K**DAPSELLR^{191}–^{77}EG**K**AMLNLLFSPR^{89}	^{181}WS**K**DAPSELLR^{191}–^{169}**K**VSELDK^{175}	
		^{181}WS**K**DAPSELLR^{191}–^{169}**K**VSELDK^{175}	^{181}WS**K**DAPSELLR^{191}–^{157}SPAGP**K**VPWFPR^{168}	
		^{184}DAP**S**ELLR^{191}–^{157}SPAGP**K**^{162}	^{181}WS**K**DAPSELLR^{191}–^{17}AVSELDA**K**QAEAIMSPR^{33}	
		^{192}**K**FR^{194} –^{278}FL**K**ER^{282}	^{181}WS**K**DAPSELLR^{191}–^{204}**K**LIAEIAFQYR^{214}	
		^{192}**K**FR^{194} –^{157}SPAGP**K**VPWFPR^{168}	^{181}WS**K**DAPSELLR^{191}–^{90}AT**K**PSALSR^{98}	
		^{192}**K**FR^{194}–^{169}**K**VSELDK^{175}	^{181}WS**K**DAPSELLR^{191}–^{39}Q**S**LIEDAR^{46}	
DNAJC12 (108-198)	Linker	^{136}K**K**EELASTAEK^{146}–^{90}AT**K**PSALSR^{98}		
		^{138}EELA**S**TAEKTEQK^{150}–^{17}AVSELDA**K**QAEAIMSPR^{33}		
		^{158}SVSPQN**S**DSSGFADVNGWHLR^{178}–^{157}SPAGP**K**VPWFPR^{168}		
	CTD	^{181}WS**K**DAPSELLR^{191}–^{77}EG**K**AMLNLLFSPR^{89}		
		^{181}WS**K**DAPSELLR^{191}–^{157}SPAGP**K**VPWFPR^{168}		
		^{181}WS**K**DAPSELLR^{191}–^{1}GPTPDATTPQA**K**^{12}		
		^{181}WS**K**DAPSELLR^{191}–^{17}AVSELDA**K**QAEAIMSPR^{33}		
		^{181}WS**K**DAPSELLR^{191}–^{222}VEYTAEEIATW**K**EVYTTLK^{240}		
		^{181}WS**K**DAPSELLR^{191}–^{459}FDP**Y**TLAIDVLDSPQAVR^{476}		
		^{181}WS**K**DAPSELLR^{191}–^{204}**K**LIAEIAFQYR^{214}		
		^{181}WS**K**DAPSELLR^{191}–^{90}AT**K**PSALSR^{98}		
DNAJC12 (176-198)	CTD	^{181}WS**K**DAPSELLR^{191}–^{7}EG**K**AMLNLLFSPR^{89}		
		^{181}WS**K**DAPSELLR^{191}–^{157}SPAGP**K**VPWFPR^{168}		
		^{181}WS**K**DAPSELLR^{191}–^{90}AT**K**PSALSR^{98}		